

Generation of ultra-broadband pulses in the near-IR by non-collinear optical parametric amplification in potassium titanyl phosphate

Oleksandr Isaienko and Eric Borguet*

Department of Chemistry, Temple University, Philadelphia, PA 19122

* Corresponding author: eborguet@temple.edu

Abstract: Non-collinear optical parametric amplification in potassium-titanyl phosphate (KTP) pumped with 800 nm pulses is reported. Broadband phase matching is achieved with non-collinear geometry and a slightly divergent signal seed. This enables a gain bandwidth up to $\sim 2500 \text{ cm}^{-1}$ in near-IR region. Introducing a chirp into the pump pulse makes it possible to amplify the white light seed in a broad spectral region from ~ 1050 to ~ 1400 nm simultaneously. Pulse compression to sub-40 fs is readily achieved, while the spectrum should support ~ 8.5 fs pulses. Angular dispersion of the broadband output is discussed.

© 2008 Optical Society of America

OCIS codes: (190.4970) Parametric oscillators and amplifiers; (190.7110) Ultrafast nonlinear optics; (320.7150) Ultrafast spectroscopy

References and links

1. C. J. Fecko, J. J. Loparo, and A. Tokmakoff, "Generation of 45 femtosecond pulses at 3 μm with a KNbO_3 optical parametric amplifier," *Opt. Commun.* **241**, 521-528 (2004).
2. G. Cirmi, D. Brida, C. Manzoni, M. Marangoni, S. De Silvestri, and G. Cerullo, "Few-optical-cycle pulses in the near-infrared from a noncollinear optical parametric amplifier," *Opt. Lett.* **32**, 2396-2398 (2007).
3. D. Brida, C. Manzoni, G. Cirmi, M. Marangoni, S. De Silvestri, and G. Cerullo, "Generation of broadband mid-infrared pulses from an optical parametric amplifier," *Opt. Express* **15**, 15035-15040 (2007).
4. S. Takeuchi and T. Kobayashi, "Broad-band near-infrared pulse generation in KTiOPO_4 ," *J. Appl. Phys.* **75**, 2757-2760 (1994).
5. T. Fuji, N. Ishii, C. Y. Teisset, X. Gu, T. Metzger, A. Baltuska, N. Forget, D. Kaplan, A. Galvanauskas, and F. Krausz, "Parametric amplification of few-cycle carrier-envelope phase-stable pulses at 2.1 μm ," *Opt. Lett.* **31**, 1103-1105 (2006).
6. C. Vozzi, G. Cirmi, C. Manzoni, E. Benedetti, F. Calegari, G. Sansone, S. Stagira, O. Svelto, S. De Silvestri, M. Nisoli, and G. Cerullo, "High-energy, few-optical-cycle pulses at 1.5 μm with passive carrier-envelope phase stabilization," *Opt. Express* **14**, 10109-10116 (2006).
7. C. P. Hauri, R. B. Lopez-Martens, C. I. Blaga, K. D. Schultz, J. Cryan, R. Chirila, P. Colosimo, G. Doumy, A. M. March, C. Roedig, E. Sistrunk, J. Tate, J. Wheeler, L. R. DiMauro, and E. P. Power, "Intense self-compressed, self-phase-stabilized few-cycle pulses at 2 μm from an optical filament," *Opt. Lett.* **32**, 868-870 (2007).
8. C. Vozzi, G. Cirmi, C. Manzoni, E. Benedetti, F. Calegari, L. Luer, G. Sansone, S. Stagira, S. De Silvestri, M. Nisoli, and G. Cerullo, "High energy self-phase-stabilized pulses tunable in the near-IR by difference frequency generation and optical parametric amplification," *Laser and Part. Beams* **25**, 471-479 (2007).
9. C. Vozzi, F. Calegari, E. Benedetti, S. Gasilov, G. Sansone, G. Cerullo, M. Nisoli, S. De Silvestri, and S. Stagira, "Millijoule-level phase-stabilized few-optical-cycle infrared parametric source," *Opt. Lett.* **32**, 2957-2959 (2007).
10. I. Nikolov, A. Gaydardzhiev, I. Buchvarov, P. Tzankov, F. Noack, and V. Petrov, "Ultra-broadband continuum amplification in the near infrared using BiB_3O_6 nonlinear crystals pumped at 800 nm," *Opt. Lett.* **32**, 3342-3344 (2007).
11. D. Kraemer, M. L. Cowan, R. Z. Hua, K. Franjic, and R. D. Miller, "High-power femtosecond infrared laser source based on noncollinear optical parametric chirped pulse amplification," *J. Opt. Soc. Am. B* **24**, 813-818 (2007).
12. A. Sugita, K. Yokoyama, H. Yamada, N. Inoue, M. Aoyama, and K. Yamakawa, "Generation of broadband mid-infrared pulses by noncollinear difference frequency mixing," *Jpn. J. Appl. Phys. Part 1* **46**, 226-228 (2007).

13. M. Tiihonen, V. Pasiskevicius, A. Fragemann, C. Canalias, and F. Laurell, "Ultrabroad gain in an optical parametric generator with periodically poled KTiOPO₄," *Appl. Phys. B* **85**, 73-77 (2006).
14. G. Cerullo and S. De Silvestri, "Ultrafast optical parametric amplifiers," *Rev. Sci. Instrum.* **74**, 1-18 (2003).
15. L. Hongjun, Z. Wei, C. Guofu, W. Yishan, C. Zhao, and R. Chi, "Investigation of spectral bandwidth of optical parametric amplification," *Appl. Phys. B* **79**, 569-576 (2004).
16. R. Butkus, R. Danielius, A. Dubietis, A. Piskarskas, and A. Stabinis, "Progress in chirped pulse optical parametric amplifiers," *Appl. Phys. B* **79**, 693-700 (2004).
17. T. Kobayashi, "Femtosecond noncollinear parametric amplification and carrier-envelope phase control," in *Femtosecond Optical Frequency Comb: Principle, Operation and Applications* (Springer, 2005), pp. 133-175.
18. D. Bodlaki and E. Borguet, "Picosecond infrared optical parametric amplifier for nonlinear interface spectroscopy," *Rev. Sci. Instrum.* **71**, 4050-4056 (2000).
19. A. Smith, "SNLO software package", retrieved February 28, 2008, <http://www.as-photonics.com/?q=SNLO>.
20. T. Kobayashi and A. Shirakawa, "Tunable visible and near-infrared pulse generator in a 5 fs regime," *Appl. Phys. B* **70**, S239-S246 (2000).
21. A. Baltuska, T. Fuji, and T. Kobayashi, "Visible pulse compression to 4 fs by optical parametric amplification and programmable dispersion control," *Opt. Lett.* **27**, 306-308 (2002).
22. S. Cussat-Blanc, A. Ivanov, D. Lupinski, and E. Freysz, "KTiOPO₄, KTiOAsO₄, and KNbO₃ crystals for mid-infrared femtosecond optical parametric amplifiers: analysis and comparison," *Appl. Phys. B* **70**, S247-S252 (2000).
23. T. D. Chinh, W. Seibt, and K. Siegbahn, "Dot patterns from second-harmonic and sum-frequency generation in polycrystalline ZnSe," *J. Appl. Phys.* **90**, 2612-2614 (2001).
24. P. Ditrapani, A. Andreoni, C. Solcia, P. Foggi, R. Danielius, A. Dubietis, and A. Piskarskas, "Matching of group velocities in 3-wave parametric interaction with femtosecond pulses and application to traveling-wave generators," *J. Opt. Soc. Am. B* **12**, 2237-2244 (1995).
25. A. Shirakawa, I. Sakane, and T. Kobayashi, "Pulse-front-matched optical parametric amplification for sub-10-fs pulse generation tunable in the visible and near infrared," *Opt. Lett.* **23**, 1292-1294 (1998).

1. Introduction

For applications such as broadband vibrational spectroscopic studies and two-dimensional IR-spectroscopy, the generation of broadband ultrashort pulses in near- and mid-IR regions of the spectrum is highly desirable [1-3]. One of the first reports of broadband generation in the ~2.1-2.6 μm region, with FWHM-bandwidth ~760 cm^{-1} , appeared as early as in 1994 [4]. Recently, several papers reported different methods for the generation of intense few-cycle pulses at wavelengths ~1.5 – 2.4 μm [5-9]. These include difference-frequency mixing (DFM) between long- and short-wavelength components of a broadband Ti-sapphire laser output to generate a seed that subsequently underwent broadband two-stage amplification in periodically poled LiNbO₃ and LiTaO₃ crystals [5]; broadband amplification of DFM-generated seed in two BBO-OPA stages at the degeneracy point [6, 8, 9]; self-phase modulation of intense ~55-fs pulses centered at 2.0 μm in a xenon filament [7]. The generation of ultra-broadband pulses at ~1.6 μm with bandwidths of ~80 – 100 THz (~2700 – 3300 cm^{-1}) also has been achieved recently from a bulk-BiB₃O₆ 800-nm pumped OPA in collinear geometry at the degeneracy point [10].

Non-collinear optical parametric wave-mixing is a promising approach for the generation of ultra-broadband radiation in the near- and mid-IR, being able to provide bandwidths of ~200-250 cm^{-1} [11, 12] or even >2100 cm^{-1} [13]. A very recent paper proposed a scheme for extension of the principles of NOPA to the near-IR wavelength region by pumping at the fundamental of a Ti-sapphire laser [2]. The experimental realization in a periodically-poled stoichiometric LiTaO₃ (PPSLT) resulted in the generation of ultra-broadband pulses covering simultaneously the ~1100-1600 nm band.

Here, we report the broadband amplification of short pulses with greater than 2500 cm^{-1} of bandwidth in the near-IR (~1050-1450 nm) by using type-II NOPA of white light pumped at 800 nm in a potassium titanyl phosphate (KTP) crystal, a nonlinear optical material which has not been previously identified for ultra-broadband generation in the IR. We show that by making the seed beam divergent at the crystal it is possible to expand the signal-idler group-velocity matching over a broad frequency range. In addition, we demonstrate the

possibility to compensate for the white-light chirp by properly stretching the pump pulses and amplifying the whole phase-matched bandwidth at once.

2. Broadband phase matching in KTP

In order to find the conditions under which broadband phase matching can be achieved in KTP, we followed the general principles of non-collinear OPA [14-17]. In particular, the bandwidth of amplified signal (idler) is inversely proportional to the group-velocity mismatch (GVM) between the signal and idler pulses (if the second- and higher order dispersion can be neglected): $\Delta\omega_s = -\Delta\omega_i \propto |1/(v_s - 1/v_i)|$. An appropriate signal-pump non-collinear geometry can equalize the signal group velocity and the projection of the group velocity of the faster idler onto the signal direction. Additionally, in order for this scheme to be achievable in a certain wavelength region, the nonlinear optical material has to possess a normal (positive) dispersion [2]. For KTP, in particular, the zero group-velocity dispersion (GVD) occurs at $\sim 1.8 \mu\text{m}$ [13], so that in the $\sim 1.0 - 1.6 \mu\text{m}$ wavelength range KTP has positive dispersion and signal-idler group-velocity matching, in principle, may be achieved.

The phase matching curves for non-collinear type-II interaction (o-pump \rightarrow o-idler + e-signal) in the xz -plane of a KTP crystal pumped at 800 nm [18], at different fixed signal-pump non-collinear angles (Fig. 1(a)) were calculated using the SNLO software package [19]. This particular parametric interaction scheme has a large nonlinear coefficient $|d_{\text{eff}}|$ (2.5 – 3 pm/V) and broad tuning range (1.0 – 4.0 μm) to allow efficient broadband amplification [18]. The geometry of interacting beams inside the crystal and the corresponding internal angles are defined in the inset of Fig. 1(a). Figure 1(b) shows GVM $\delta_{si} = [1/(v_i \cos(\alpha + \beta)) - 1/v_s]$ between signal and idler projection onto the signal direction, calculated at different values of α .

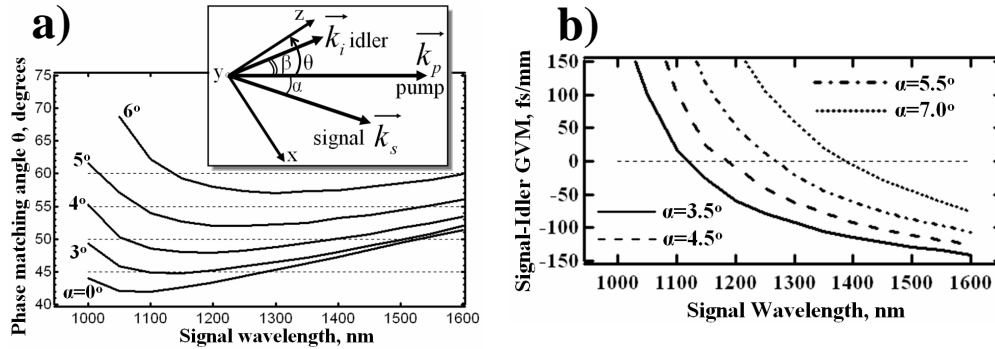


Fig. 1. (a). Phase matching curves for OPA in KTP (xz -plane, type II, e-signal + o-idler=o-pump) at different non-collinear angles between 800-nm pump and seed. Inset: internal geometry of the three interacting beams with respect to the crystal axes: z – optical axis; α , β – signal-pump and idler-pump non-collinear angles, respectively; θ – phase matching angle between pump and optical axis. (b). Signal-idler GVM δ_{si} at different α .

Although there is no single phase matching curve with broad flat region (as exists for BBO in the visible [20]), at $\alpha \approx 4-5^\circ$ it is possible to phase match a set of curves corresponding to different seed-pump non-collinear angles. This behavior suggests the possibility to amplify a large bandwidth of signal frequencies if the signal seed beam is not collimated but rather diverges in the crystal.

3. Experimental results

The experimental setup for ultra-broadband KTP-NOPA is shown in Fig. 2. The source for the pump beam is a Coherent Ti-sapphire oscillator and Alpha BMI-Coherent regenerative amplifier operating in fs-mode, described elsewhere [18]. 260 μJ ~ 150 fs 800-nm pulses at

repetition rate of 1 kHz are split by a combination of a half-wave plate (HW1) and polarizer-beam-splitter (PBS) into two parts. $\sim 5 \mu\text{J}$ is focused with a 100-mm lens (L1, BK7) into a 2-mm thick sapphire plate (S) for WL-seed generation. The WL-beam is collimated with a 45-mm lens (L2, BK7) and focused into the KTP crystal with a 250-mm lens (L3, BK7). The remaining pump beam ($\sim 250 \mu\text{J}$) is first sent into a system of half-wave plates and prisms for pulse stretching in order to compensate for possible chirp in WL-seed and to reduce the pump peak intensity to below the damage threshold of KTP [21].

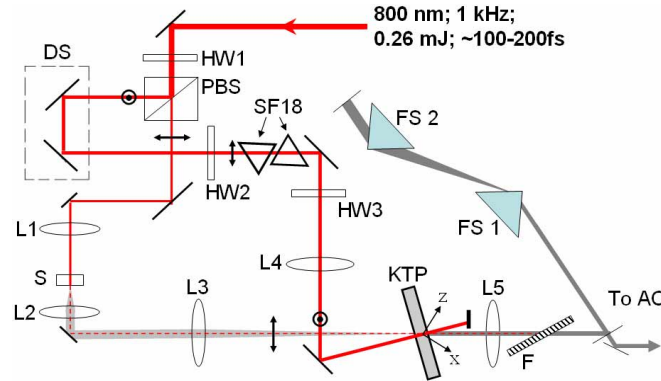


Fig. 2. Experimental setup: HWP, half-wave plate; PBS, polarizer-beamsplitter; DS, delay stage; SF18, equilateral prisms; S, 2-mm sapphire plate; L, BK7 lenses; FS, 69.06°-apex angle fused silica prisms; F, long-pass filter for blocking $\lambda < 1000 \text{ nm}$; AC, autocorrelator. Also shown is the zx -plane of KTP. Double arrows and circled dots represent polarization in the plane of and perpendicular to the drawing, respectively.

In order to stretch the pump pulses, we used two equilateral SF18 prisms (face size 25 mm) oriented at Brewster's angle with respect to the pump beam. The adjacent faces of the two prisms are parallel to each other. The half-wave plate (HW2) makes the pump beam p-polarized at the prism surfaces, and another half-wave plate (HW3) rotates the pump polarization to ordinary for parametric amplification in the KTP-crystal. The insertion of the prisms and distance between them were adjusted to optimize the stretched pulse duration. The pump pulse width was measured by picking the beam before the stretcher system and after it with a home-built autocorrelator with a 0.5-mm BBO crystal. Autocorrelation measurements of the pump pulsewidth before and after the HW2-SF18-SF18-HW3 system showed that the two SF18 prisms provide enough GVD to stretch ~ 12 -nm broad 800 nm pulses from ~ 180 fs to >500 fs. After stretching, the pump beam is focused into the KTP crystal with a 300-mm lens (L4, BK7). The power of the pump right before the KTP is $\sim 150 \text{ mW}$ (we relate the $\sim 40\%$ losses to reflections at surfaces of the optics), and the focal point is adjusted to be $\sim 4 \text{ cm}$ behind the crystal. The estimated pump pulse intensity is $\sim 270 \text{ GW/cm}^2$, below the reported damage threshold [22]. The 2-mm thick KTP crystal is cut at $\theta=42^\circ$, $\phi=0^\circ$ (initially it was cut for a collinear OPA). The external angles of incidence for pump and seed beams at the KTP-crystal surface are 12° and 18.8° , respectively. We calculated the internal phase matching angles for pump and seed beams to be 48.8° and 52.6° , respectively, and $\alpha \sim 4.0^\circ$. The amplified signal is collimated with a 150-mm lens (L5, BK7) and compressed in a fused-silica prism pair compressor with $\sim 24 \text{ cm}$ inter-prism separation.

The amplified signal pulses were characterized by recording second-harmonic generation (SHG) spectra off the surface of a 2-mm thick polycrystalline ZnSe-crystal (P-ZnSe) [23] with a CCD-camera. P-ZnSe has shown high-efficiency doubling in the $\sim 1000 - 1600 \text{ nm}$ wavelength region [23] and has insignificant phase-matching restrictions on the converted bandwidth. A similar spread of visible wavelengths was generated by doubling the signal pulses in the 0.5-mm thick BBO (gradually rotated around its axis as phase matching for all

wavelengths present in the ultrabroadband pulse was not simultaneously possible). This excludes 1- or 2-photon fluorescence from ZnSe as the source of the observed spectra. The SHG-spectra were processed as follows: the background was subtracted, square root of intensity was taken (with assumption that at each wavelength the intensity of SHG is proportional to the square of fundamental), and the wavelength scale was doubled.

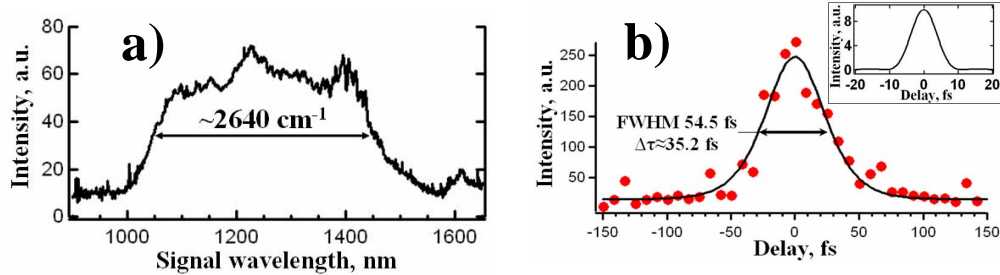


Fig. 3. (a) Typical spectrum of the full-bandwidth NIR-signal derived from SHG-spectrum off P-ZnSe-surface (see text). We relate the feature at ~ 1600 nm to imperfect filtering of 800-nm seed component. (b). Autocorrelation of signal on 30- μm -BBO crystal (FWHM 54.5 fs, sech^2 -pulsewidth ~ 35.2 fs). Inset: Intensity time-profile of the Fourier transformed spectrum.

A typical spectrum (Fig. 3(a)) of the NIR-signal of the NOPA shows a FWHM ~ 400 nm (~ 2600 cm^{-1} or ~ 78 THz). The output power of the NIR-signal is $\sim 3\text{--}4$ mW in full-bandwidth operation, corresponding to $>2\%$ conversion efficiency. The autocorrelation of the signal beam in a 30- μm BBO crystal (Fig. 3(b)) is ~ 55 fs corresponding to a pulsewidth of 35 fs assuming a sech^2 -pulse shape, while the spectrum supports ~ 8.5 fs transform-limit pulses as demonstrated by Fourier transform of the spectrum (inset in Fig. 3(b)). As a first approximation, the spectrum can be modeled as a rectangular pulse (corresponding to sinc^2 -shape in the time domain), suggesting that the shortest experimentally achievable pulse durations would be ~ 10 fs. A more sophisticated approximation would be to model the pulse as resulting from a trapezoid like electric field, reproducing both the curved wings and flat top of the spectrum in Fig. 3(a). The corresponding pulse width is ~ 8 fs. This latter approximation is consistent with the direct Fourier transform, without assumptions on the pulse shape, yielding ~ 8.5 fs pulsewidth.

4. Discussion

In order to explain our results, we considered the divergence of the seed beam at the KTP-crystal. After collimation with lens L2, the seed beam has ~ 7 mm diameter, providing a full-angle divergence of $\sim 1.6^\circ$ (when focused with a 250-mm lens) corresponding to the internal full-angle divergence of $\sim 0.86^\circ$, so that $\alpha \approx 4.0^\circ \pm 0.43^\circ$, or $\alpha \approx [3.5^\circ \dots 4.4^\circ]$. The calculated phase matching curves at $\alpha = 3.5^\circ$, 4.0° , and 4.4° are shown in Fig. 4. Also shown is the pump phase matching angle $\theta = 48.8^\circ$ (the internal full-angle divergence of the pump, $< 0.35^\circ$, is neglected). As one can see, the boundaries of wavelength region where the signal seed is phase matched are determined by intersections of the $\theta = 48.8^\circ$ line with the $\alpha = 3.5^\circ$ curve. From Fig. 4, it follows that the signal is expected to be amplified simultaneously within $\sim 1050\text{--}1400$ nm range, which is consistent with experimental results (Fig. 3(a)), although there is some discrepancy between these values of α and those for which GVM=0 is achieved (Fig. 1(b)).

The fact that compression of signal pulses closer to transform limit could not be reached, cannot be explained just by insufficient compensation of the third and higher order dispersions. Such a long autocorrelation is a result of angular dispersion of the signal, which was not compensated for in the current setup. One of the causes for the angular dispersion is the divergence of the WL-seed at the crystal ($\sim 0.86^\circ$) which may cause amplification of different wavelength components at different exit angles (Fig. 4). Another reason, which may be even

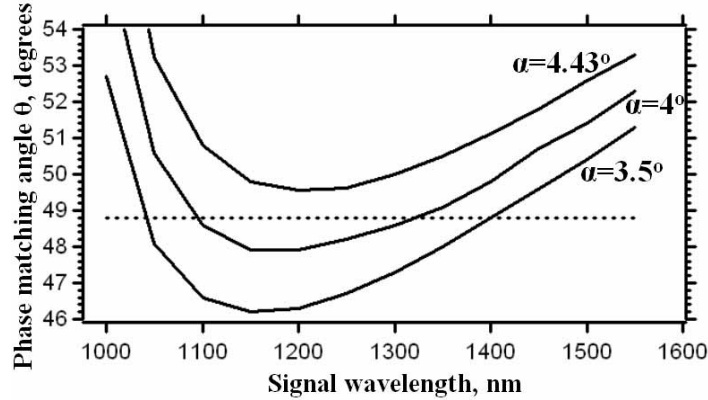


Fig. 4. Phase matching curves for non-collinear OPA in KTP (xz-plane, type II, e-signal + o-idler = o-pump) at signal-pump non-collinear angles 3.5°, 4.0° and 4.43°. The dashed line represents the direction of the pump beam in the KTP crystal ($\theta=48.8^\circ$).

more detrimental, is the pulse-front tilting of the signal during non-collinear interaction with the pump pulses [17, 20, 24, 25]. According to [20], the internal pulse-front tilt angle of the signal is expected to be $\gamma_{\text{int}} = \alpha \approx 3.5\text{-}4.0^\circ$, resulting in a large external tilt angle $\gamma_{\text{ext}} \approx 6.4 - 7.3^\circ$ upon the exit from the KTP-crystal (relation $\tan(\gamma_{\text{int}}) = \tan\alpha = (v_s/c)\tan(\gamma_{\text{ext}})$ was used; $v_s=c/1.8196$ for $\sim 1300\text{-nm}$ centered e-signal). We believe that the signal angular dispersion caused by the pulse-front tilt can be removed by tilting the pump pulses by a proper angle [20]. Compensation of effects introduced by the divergence of the seed beam, however, may require more complicated approaches (e.g. use of micromachined mirrors [21]). The characterization of the signal angular dispersion and preparation of the setup for its compensation are currently in progress.

In conclusion, we have demonstrated broadband parametric amplification in a KTP crystal with $>2500\text{-cm}^{-1}$ bandwidth in the near-IR region by employing non-collinear phase matching with a slightly divergent seed beam. To our knowledge, this is the first report of ultra-broadband generation in the near-IR implemented experimentally in bulk KTP (as opposed to periodically-poled KTP [13]). Use of chirped pump pulses enabled simultaneous amplification of the whole phase-matched bandwidth. With the proper correction of the signal pulse-front and pulse compression, generation of sub-10 fs near-IR pulses should be achievable.

Acknowledgments

This work was supported by DOE-Office of Basic Energy Sciences. The authors thank the Levis group for the use of a 30- μm BBO crystal for autocorrelation measurements.